

Oscillating red giants in the CoRoT^{*} exo-field: Asteroseismic mass and radius determination

Thomas Kallinger¹, Werner W. Weiss¹, Caroline Barban², Frédéric Baudin², Fabien Carrier³, Joris De Ridder³,
Artie Hatzes⁴, Saskia Hekker^{5,3}, and Magali Deleuil⁶

¹ Institute for Astronomy, University of Vienna, Türkenschanzstrasse 17, 1180 Vienna, Austria

² Observatoire de Paris, LESIA, CNRS UMR 8109 Place Jules Janssen, F-92195 Meudon, France

³ Instituut voor Sterrenkunde, Katholieke Universiteit Leuven, Celestijnenlaan 200 B, 3001 Heverlee, Belgium

⁴ Thüringer Landessternwarte Tautenburg, Sternwarte 5, 07778 Tautenburg, Germany

⁵ Royal Observatory of Belgium, 1180 Brussels, Belgium

⁶ Laboratoire d'Astrophysique de Marseille (UMR 6110), Technopole de Marseille-Etoile, F-13388 Marseille cedex 13, France

Received 2008 ; accepted ???

ABSTRACT

Context. Observations and analysis of solar-type oscillations in red giant stars is an infant field of asteroseismic research with a number of open questions. Although stochastic oscillations have been firmly detected in red giants, both in radial velocity and photometric time series, the mostly too short or incomplete data sets complicate a detailed analysis. The french-led satellite CoRoT induced a breakthrough in observing *p*-mode oscillations in red giants. We have analyzed continuous photometric time series of about 11 400 relatively faint stars obtained in the *exofield* of CoRoT during the first 150 days long-run campaign from May to October 2007. Among them, we found more than 300 stars showing a clear power excess in a frequency and amplitude range where it can be expected for red giant pulsators. In this paper we present first results on a sub-sample of these stars.

Aims. The knowledge of reliable fundamental parameters is essential for detailed asteroseismic studies of red giant stars. As the CoRoT *exofield* targets are relatively faint (11–16 mag) no or only weak constraints can be set on their location in the HR-diagram. We therefore aim to extract information about fundamental parameters from the available time series alone.

Methods. We model the convective background noise and the power excess hump due to pulsation with a multi-component fit and deduce reliable estimates for the stellar mass and radius from scaling relations for the frequency of maximum power and the characteristic frequency separation.

Results. We provide a simple method to estimate stellar mass and radius for stars showing solar-type oscillations and test our approach for a number of well-known solar-type pulsators. We apply the method to our sample of CoRoT red giants and provide their mass and radius as a starting point for a more detailed model analysis.

Key words. stars: oscillations – stars: fundamental parameters – techniques: photometric

1. Introduction

Stars cooler than the red border of the instability strip have convective envelopes with turbulent motions on various time scales and velocities up to the speed of sound. This acoustic noise in the star's resonant cavity may drive intrinsically stable *p*-mode pulsation, so-called damped and stochastically excited (or solar-type) oscillations. All cool stars with convective outer layers potentially show solar-type oscillations with typically small amplitudes, which hamper their detection in main-sequence and sub-giant stars. But as amplitudes are believed to scale with the luminosity, they should therefore be easier to observe in the more evolved red giants which opens up a promising potential for asteroseismic investigations. Their larger radii, however, adjust the pulsation periods from minutes to several hours to days. This in turn complicates ground-based detection and calls for long and uninterrupted observations from space.

The satellite CoRoT (Baglin, 2006) is continuously collecting white light high-precision photometric observations for 10 bright stars in the so-called *seismo*field as well as 3 color photometry for thousands of relatively faint ($11 \leq m_V \leq 16$ mag) stars in the so-called *exofield*. The primary goal of the latter is to detect planetary transits. But the data are also perfectly suited for asteroseismic investigations. And indeed, a first processing of the first CoRoT *exofield* data reveals a variety of oscillating red giants. De Ridder et al. (2008, hereafter paper I) report on the clear detection of solar-type pulsation in about 300 red giants among the ~11 400 stars continuously observed during the first 150 days CoRoT long-run (LRc01) campaign.

In paper I, the debate on the existence of non-radial modes in red giants with moderate mode lifetimes versus the presence of short living radial modes only is discussed. Barban et al. (2007) interpreted the signal found in the 28 days of continuous MOST observations of the G9.5 giant ϵ Oph as radial modes with relative broad modes profiles corresponding to short mode lifetimes of ~2.7 days. This result was consistent with what was found for the similar red giant ξ Hya (Stello et al., 2006). On the other hand, Kallinger et al. (2008) re-examined the MOST photometry of ϵ Oph and found at least 18 radial *and* non-radial modes with significantly longer mode lifetimes (10 - 20 days) which are

Send offprint requests to: kallinger@astro.univie.ac.at

* The CoRoT (*Convection, Rotation, and planetary Transits*) space mission, launched on 2006 December 27, was developed and is operated by the CNES, with participation of the Science Programs of ESA, ESAs RSSD, Austria, Belgium, Brazil, Germany and Spain.

consistent with frequencies of a red giant model that lies within the $\pm 1\sigma$ uncertainty box of ϵ Oph’s position in the HR-diagram. In paper I, we give clear evidence for regular p -mode patterns of radial and non-radial modes with long lifetimes for at least two red giants investigated so far.

The low-degree, high-radial order p -modes reported for several main sequence and sub-giant stars allow detailed asteroseismic studies based on the observed frequencies only. Their characteristic frequencies separations, such as the large and small frequency spacing, are large compared to the observational uncertainties. It should therefore be easier to compare the observed frequencies with those determined from theoretical models. Even small deviations from the asymptotic relation, dedicated to more local phenomena in the stellar interior, are accessible in some cases. Not so for the more evolved stars on the giant branch. Their characteristic frequency separations are significantly smaller and at a certain point are comparable to the observational uncertainties. This complicates considerably the asteroseismic analysis. It is thus of essential interest to constrain the parameter space for the models by using reliable fundamental parameters. Apart from pulsation, red giants also show, e.g., significant power from the turbulent fluctuations in their convective envelopes which offer the possibility to study the convective time scales and amplitudes. But all this is of less relevance without the knowledge where to place a star in the HR-diagram, which knowledge is indeed lacking for most of the faint CoRoT *exofield* stars. The available broadband color information may allow in some case to roughly estimate the effective temperature but is not suitable to distinguish giants from main sequence stars. We therefore try to extract the fundamental parameters from the time series alone, which is the main topic of this paper. We model the convective background noise and the power excess due to pulsation with a multi-component fit which allows us to determine the so-called frequency of maximum power, the frequency at which the pulsation power excess is centered on. With this and the large frequency separation we derive the stellar mass and radius from well-known scaling relations. As a first estimate we also obtain effective temperatures and luminosities from a comparison with evolutionary tracks.

At the end we state that we will continue the determination of fundamental parameters in a subsequent paper by using the dependence of the total pulsation power excess in the power density spectrum on the stellar luminosity. In the future, we will also provide an online database for pulsating red giants observed in the CoRoT *exofield* as well.

2. Observations

Although the CoRoT satellite and the *exofield* data are well explained in paper I, we will briefly summarize the instrument and data sets.

CoRoT houses four $1 \times 1K$ pixels CCD photometers fed by a 27-cm afocal telescope. The satellite’s low-Earth polar orbit (period ≈ 100 min) enables uninterrupted observations of stars in its Continuous Viewing Zones (two cones with $\sim 10^\circ$ radius centered on the galactic plane at right ascension of about 6:50 h and 18:50 h, respectively) for up to 6 months. A summary of the mission is given in the pre-launch proceedings of CoRoT published by ESA (SP-1306, 2006). The two core science objectives, asteroseismology across the HR-diagram and the detection of transiting extra-solar planets, are tracked simultaneously with 2 of the 4 detectors each, the *seismofield* and *exofield* CCDs. In order to check the color independency of presumed planetary transits, the stellar light is dispersed by a prism before it reaches

the *exofield* detectors. In this paper we concentrate on the white light flux measurements. These are obtained by adding the flux of the three color channels and improve the photometric quality.

During the first 150 days long-run campaign, CoRoT pointed towards the coordinates $(\alpha, \delta) = (19.4\text{h}, 0.46^\circ)$ from May to October, 2007, and gathered time series for about 11 400 stars sampled with a cadence of either 512 s or 32 s, depending on the predefined status of the star (the limited downlink capacity does not allow to sample all stars with the short cadence). There is, however, the so-called alarm mode, where stars originally measured in the long cadence are switched to the short cadence after a few days of observations if they turn out to be “interesting”. Typically, each time series consists of about 25 000 respectively 400 000 data points with a duty cycle of about 90%. We use the N2 data format, which is the output of a standard data reduction procedure, and detect and remove occasional jumps in the time series (caused by high energy particles) and apply an outlier correction. In a next step, we compute Fourier amplitude spectra of all time series and extract parameters which we believed to be characteristic for red giant pulsators, like the $1/f^2$ characteristic or the existence of a power excess hump. Based on a pre-selection with these parameters, we use a semi-automatic routine to identify the pulsating red giants. A more detailed description of how to identify the red giant stars will be given in Hekker et al. (in preparation).

3. Power spectra modeling

The detection and analysis of stellar observations is significantly complicated in stars cooler than the red border of the instability strip due to the turbulent motions in the convective envelopes which superpose the oscillations on similar time scales. The temporal evolution and rotational modulation of structures on the stellar surface causes stochastic variations which generates significant power in frequency ranges typical for solar-type pulsa-

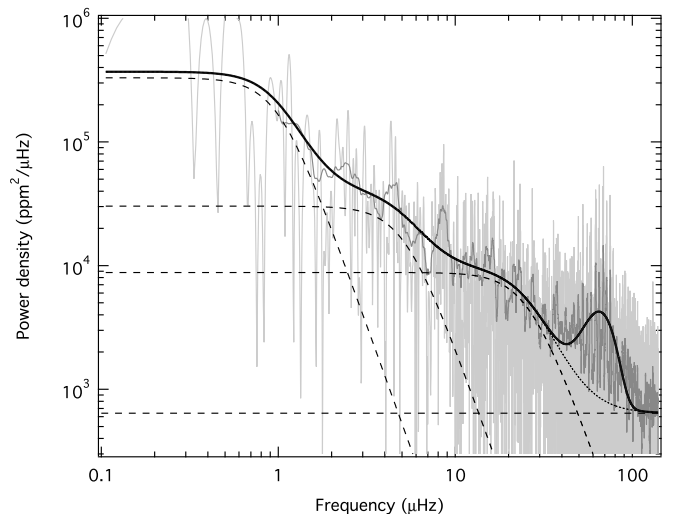


Fig. 1. Power density spectrum of the CoRoT *exofield* photometric time series of the pulsating red giant “B” and a multi-component function (black line) fitted to the heavily smoothed power density spectrum. The function is a superposition of white noise (horizontal dashed line), three power law components (dashed lines) and a power excess hump approximated by a Gaussian function. The dark-grey line indicates a smoothed version of the original power spectrum.

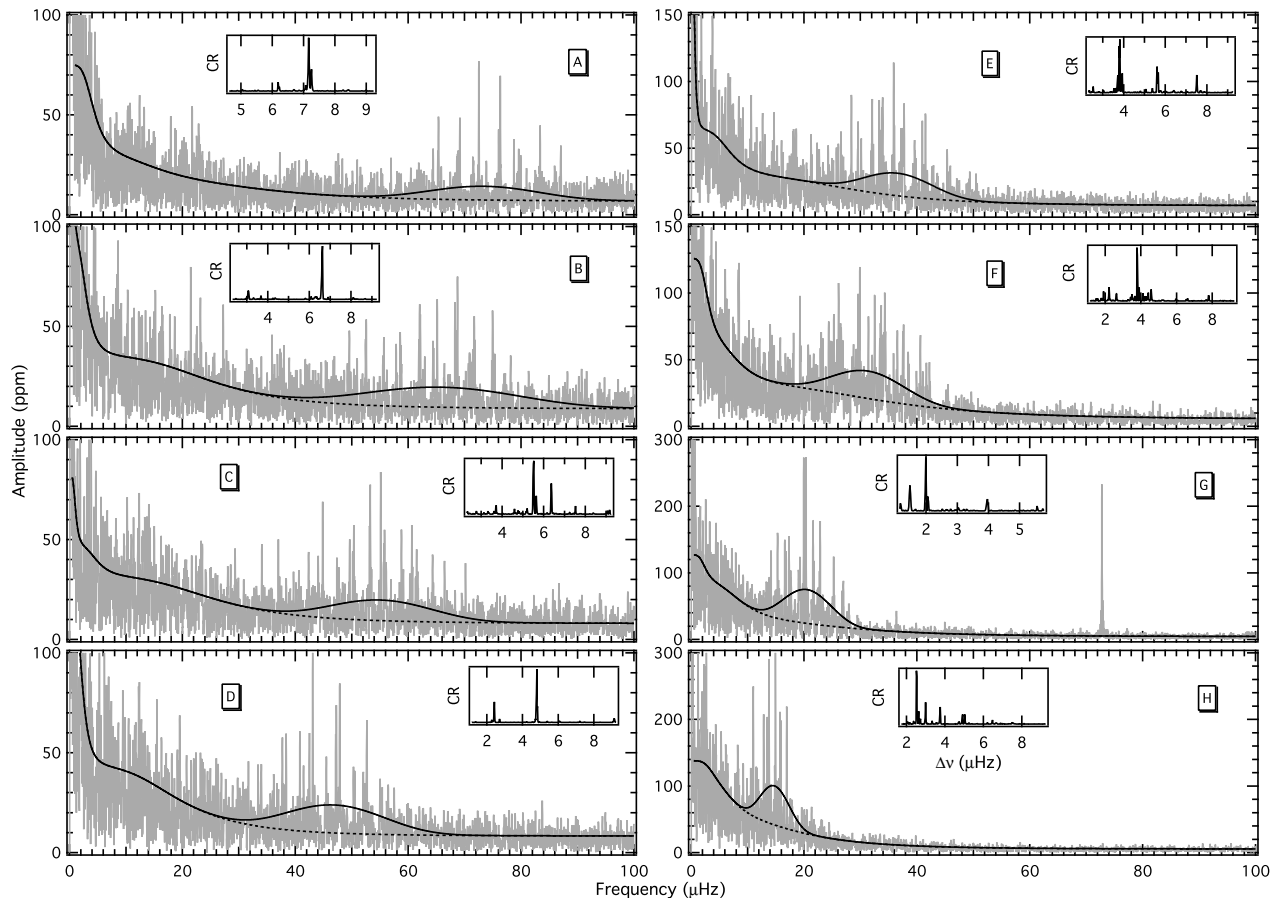


Fig. 2. Fourier amplitude spectra of a sample of CoRoT oscillating red giants. Black lines correspond to a multi-component function (see text) fitted to the power spectra. Dotted lines represent the power law part only. The center of the pulsation power excess hump, approximated by a Gaussian function, is adopted to be the frequency of maximum power. Inserts give the Comb response function used to determine the large frequency separation.

tion. This additional power may affect the accurate determination of oscillation frequencies, amplitudes, and lifetimes.

Although the turbulent motions on the surface are stochastic, they follow particular characteristics. It can be shown that stochastic variations on time scales longer than the sampling rate of the observations cause correlations of consecutive measurements with the strength of the correlations exponentially decreasing for increasing time-lags. The Fourier transform of such a correlated “noise” is in turn a Lorentzian profile (centered on frequency equal to zero), characterized by an amplitude and a characteristic frequency or time scale. The latter reflect the general properties of the convective process. For the Sun, it is common practice to model the background signal with power laws to allow accurate measurements of solar oscillation frequencies and amplitudes. Power law models were first introduced by Harvey (1985) and Aigrain et al. (2004). Only recently Michel et al. (2008) use the sum of power laws: $P(\nu) = \sum_i P_i$, with $P_i = a_i \zeta_i^2 \tau_i / (1 + (2\pi\tau_i\nu)^{C_i})$, or hereafter $P_i = A_i / (1 + (B_i\nu)^{C_i})$, to fit the solar background, with ν being the frequency, τ_i the characteristic time scale, and C_i the slope of the power law. a_i serves as normalization factor for $\zeta_i^2 = \int P_i(\nu) d\nu$ which corresponds to the variance of the stochastic variation in the time domain. The slope of the power laws was originally fixed to 2 in Harvey’s models but Aigrain et al. (2004) have shown that, at least for the Sun, the slope is closer to 4. The number of power

law components, i , usually varies from two to five, depending on the frequency coverage. Each power law component represents a different class of physical processes such as stellar activity, activity of the photospheric/chromospheric magnetic network, or granulation (see Aigrain et al. 2004 or Michel et al. 2008 and references therein) with time scales for the Sun ranging from months for active regions to minutes for granulation.

Compared to the Sun, the variance of the granulation signal and its time scale in red giants scale with the extended radius. More detailed, Stello et al. (2007) have shown in their analysis of pulsating red giants in M67 that it can be assumed that the granulation cell size is proportional to the pressure scale-height in the atmosphere and the variance of the granulation is inversely proportional to the number of cells on the stellar surface. Furthermore, they estimated the granulation time scale to be defined by the ratio between the size of the granules and their velocities which in turn is assumed to scale with the sound speed in the atmosphere.

First tests with power law fits to the CoRoT photometry have shown that the presence of a pulsation power excess in a frequency range close to characteristic frequencies of the power laws significantly influence the fit. We therefore model the observed power spectrum with a superposition of white noise, the

sum of power laws¹, and a power excess hump approximated by a Gaussian function:

$$P(\nu) = P_n + \sum_i \frac{P_i}{1 + (B_i \cdot \nu)^4} + P_g \cdot e^{-(\nu_{\max} - \nu)^2 / (2\sigma^2)}, \quad (1)$$

where P_n represents the white noise contribution and P_i and B_i are the amplitudes of stellar background components and their characteristic time scales, respectively. P_g , ν_{\max} , and σ are the height, the central frequency and the width of the power excess hump, respectively. We fit the resulting multi-component function to the smoothed power spectra by using a Levenberg-Marquardt least-squares algorithm to determine the 10 (or 8) free parameters. As an example, we show in Figure 1 the power density spectrum of one of our program stars (grey line) along with the resulting multi-component fit (black line). The spectral power density measures the power per frequency resolution element, which automatically makes it independent of the length and sampling function of the time series. We use the total area under the spectral window, which is about $0.091 \mu\text{Hz}$, to convert power to power density. For the red giant shown in Figure 1, the white noise is about $640 \text{ ppm}^2 / \mu\text{Hz}$. The power law components have time scales of about 12, 3.7, and 0.5 days and the power excess hump is centered on $65.3 \mu\text{Hz}$ and has a height and width of $\sim 3200 \text{ ppm}^2 / \mu\text{Hz}$ and $\sim 12.2 \mu\text{Hz}$, respectively.

Figure 2 shows a sequence of amplitude spectra selected from 31 red giant pulsators (out of the ~ 300 identified) analyzed so far with the corresponding fits. Note that the fits are calculated in power but are presented in amplitude (for better visibility). This sequence of red giant amplitude spectra nicely demonstrates that the frequency ranges of pulsation and granulation, as well as their amplitudes, scale simultaneously with the global stellar parameters. The fit without the Gaussian component (dotted lines in Figure 1 and 2) can be used to estimate the local background noise and allows us to accurately determine oscillation frequencies and amplitudes and to rate their signal-to-noise ratio. But more interesting in this context, the Gaussian component locates the center of the power excess hump, an important asteroseismic parameter known as the frequency of maximum power.

4. Asteroseismic determination of fundamental parameters

The amplitudes of solar oscillations are modulated by a broad envelope with its maximum at a frequency of about 3 mHz. The center and the shape of the envelope is defined by the excitation and damping, where the latter can be assumed to be Gaussian (see previous section). Kjeldsen & Bedding (1995) have shown that the frequency of maximum power, ν_{\max} , of p -mode oscillations scales to good approximation with the acoustic cutoff frequency, which sets limits on the maximum frequency for acoustic oscillations. Since the acoustic cutoff frequency also defines a typical atmospheric time scale, they argue that ν_{\max} should scale with the acoustic cutoff to $\nu_{\max} \propto c_s / H_p$, with c_s being the speed of sound and $H_p \propto T/g$ the pressure scale height of the atmosphere. In the adiabatic case and under the assumption of an ideal gas, ν_{\max} is then $\propto g / \sqrt{T_{\text{eff}}}$. They then predict the frequency of maximum power to scale from the solar case as:

$$\nu_{\max} = (M/M_{\odot}) \cdot (R/R_{\odot})^{-2} \cdot (T_{\text{eff}}/5777 \text{ K})^{-1/2} \cdot 3050 \mu\text{Hz} \quad (2)$$

¹ The number of components is generally set to three in some cases only two – when it was necessary to remove instrumental jumps which significantly affects the very low frequency range

We derive ν_{\max} directly from the power spectra as the central frequency of the Gaussian part of our multi-component fit as given by Eq. 1.

Another characteristic parameter that can directly be derived from the observed power spectrum is the asymptotic large frequency separation, $\Delta\nu$, of consecutive overtones of same spherical degree. The large frequency separation, which is about $134.9 \mu\text{Hz}$ for the Sun (Toutain & Fröhlich, 1992), is determined by the inverse profile of the sound speed to $\Delta\nu \propto (2 \int_0^R dr/c_s)^{-1}$. Since the adiabatic speed of sound is proportional to the square root of the ideal gas temperature, $\Delta\nu \propto \sqrt{\langle T \rangle} / R$, where $\langle T \rangle$ is the average internal temperature which can be assumed to scale with M/R . Doing so, $\Delta\nu$ is thus $\propto (M/R^3)^{1/2}$, hence directly proportional to the mean stellar density and scales from the solar case (Cox, 1980) as:

$$\Delta\nu = (M/M_{\odot})^{1/2} \cdot (R/R_{\odot})^{-3/2} \cdot 134.9 \mu\text{Hz} \quad (3)$$

We determine $\Delta\nu$ from the Comb-response (CR) function (Kjeldsen et al., 1995) of the observed power spectra in the frequency range of pulsation, $\nu_{\max} \pm 3\sigma$. The CR function probes characteristic frequency spacings for the asymptotic regime in p -mode oscillation spectra and is given in the inserts of Figure 2 with arbitrary ordinates.

Knowing ν_{\max} and $\Delta\nu$ (and T_{eff}), it is now easy to derive the stellar mass and radius:

$$R/R_{\odot} = (\nu_{\max}/\nu_{\max,\odot}) \cdot (\Delta\nu/\Delta\nu_{\odot})^{-2} \cdot \sqrt{T_{\text{eff}}/5777 \text{ K}} \quad (4)$$

$$M/M_{\odot} = (R/R_{\odot})^3 \cdot (\Delta\nu/\Delta\nu_{\odot})^2 \quad (5)$$

We have tested this method for a number of well-known solar-type pulsators and compare stellar radius and mass based on our approach with values found in the literature in Table 1. Note, ν_{\max} and $\Delta\nu$ of β Oph are based on unpublished MOST photometry. ν_{\max} of ξ Hya is derived from a weighted average of the published frequencies. ν_{\max} and $\Delta\nu$ of β Hyi and α Cen A

Table 1. Mass and radius of stars used to test our mass and radius determination approach. M and R are calculated without the temperature term in Eq. 4, if no effective temperature is given.

	ν_{\max} [μHz]	$\Delta\nu$	T_{eff} [K]	this work		literature	
				R	M	R	M
				----- solar units -----			
β Oph ^a	46.0	4.1	-	14.8	3.0	12.2	3.2
ϵ Oph ^b	53.5	5.2	-	10.7	1.82	10.8	2.02
ξ Hya ^c	92.3	7.0	-	10.2	2.85	10.4	3.07
η Ser ^d	125.0	10.1	-	6.6	1.63	6.3	1.6
M67 13 ^e	208.9	15.9	4870	4.6	1.32	4.3	1.35
ν Ind ^f	~ 320	24.5	5300	3.04	0.93	2.97	0.85
ζ Her A ^g	~ 700	~ 43	5830	2.27	1.19	2.51	1.3
α CMi ^g	~ 970	~ 54	6530	2.11	1.51	2.08	1.5
β Hyi ^h	~ 1000	56.2	5800	1.89	1.17	1.87	1.1
μ Ara ⁱ	~ 1900	~ 90	5810	1.40	1.23	1.38	1.18
α Cen A ^j	~ 2300	~ 106	5770	1.22	1.12	1.22	1.11
α Cen B ^j	~ 4000	~ 161	5300	0.88	0.98	0.86	0.93

^a Simbad, CDS

^b Kallinger et al. (2008)

^c Frandsen et al. (2002)

^d Hekker et al. (2006)

^e Stello et al. (2007)

^f Carrier et al. (2007)

^g Martic et al. (2001)

^h Bedding et al. (2001)

ⁱ Bouchy et al. (2005)

^j Eggenberger et al. (2004)

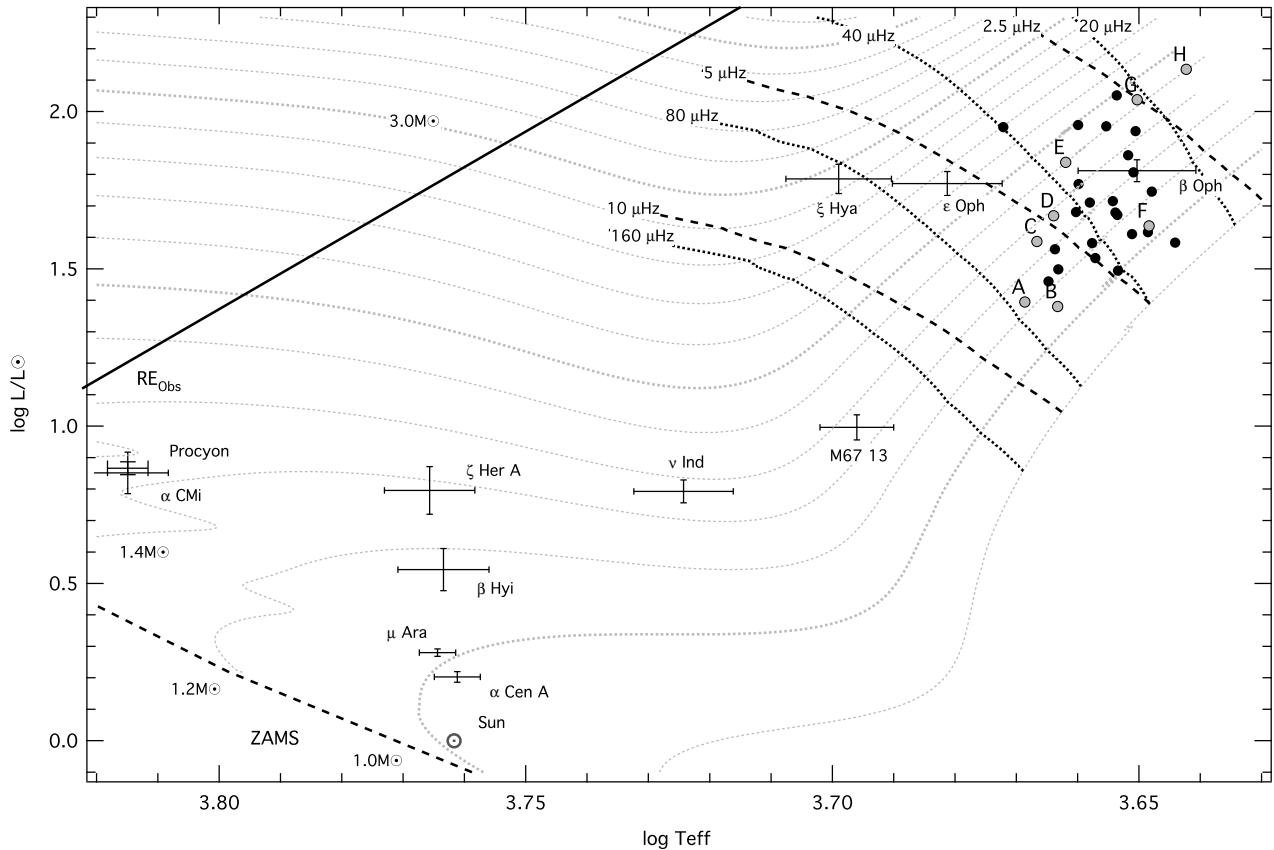


Fig. 3. Theoretical HR-diagram showing the location of the stars used to test our mass and radius determination approach. Black dots (total sample of the analyzed stars) and grey-filled dots (stars presented in Figure 2) indicate the CoRoT pulsating red giants based on a comparison with YREC evolutionary tracks. Dashed black lines give isopleths for $\Delta\nu = 2.5, 5, \text{ and } 10 \mu\text{Hz}$. Dotted black lines give isopleths for $\nu_{\text{max}} = 20, 40, 80, \text{ and } 160 \mu\text{Hz}$.

& B are taken from Kjeldsen et al. (2005). Although ν_{max} is in some cases only a rough estimate from published power spectra, our approach yields quite accurate estimates for mass and radius in a large portion of the HR-diagram. E.g., the well-known mass and radius of α Cen A are within 1% in mass and 3% in radius, respectively, compared to our values.

However, there are no reliable effective temperatures available for our sample of CoRoT red giants and it seems, one cannot use this method. But as ν_{max} depends only on the square root of T_{eff} and pulsating red giants are expected to populate only a relatively narrow temperature range (~ 4200 to 5300 K) it is justified to fix T_{eff} to an average value of 4750 K. The resulting internal error from this approach is not larger than $\sim 6\%$ for the radius and $\sim 19\%$ for the mass and, hence, still a reasonable estimate. Although there are reliable temperature estimates available for the first 4 stars listed in Table 1 we ignore them and use the average temperature for red giants to determine their mass and radius. We list the thus derived radius and mass values for our preliminary sample of 31 red giants in Table 2 along with the frequencies of maximum power and large frequency separations.

To estimate the position in the HR-diagram of these stars we identified solar calibrated models of same radii and mass falling along evolutionary tracks computed with the Yale Stellar Evolution Code (YREC; Guenther et al., 1992; Demarque et al., 2007). In Figure 3 we show the interpolated effective temperatures and luminosities of our sample of stars along with the positions of the test stars (Table 1). To compute the evolutionary tracks, the initial helium and metal mass fraction was set to (Y,

Z) = (0.28, 0.02). A mixing length parameter of $\alpha=1.8$ is used to meet the Sun's position in the HR-diagram with a 1 solar mass model at roughly the solar age. A more detailed description of the used model physics can be found in Kallinger et al. (2008) or Kallinger (2008). In Figure 3 also contours of constant ν_{max} and $\Delta\nu$ are given. Note that they are specific to the presented model grid. They will slightly move when changing for instance the primordial composition of the tracks. We also note that we do not give error bars for the effective temperature and luminosity estimates (Table 2) because both values depend on the specific parameters of the stellar model. They should only indicate where to expect a given star in the HR-diagram.

5. Conclusions and prospects

We have shown that global properties of solar-type pulsation can be used to derive reliable estimates for stellar mass and radius by employing well established and often used scaling relations. We have tested this approach on various prominent solar-type pulsators and applied it to a first sample of red giant pulsators observed by CoRoT. Despite the mentioned approximations the derived fundamental parameters can serve to constrain the starting values for a more detailed analysis.

We note that we do not stop at this point. In a next step we will use the integral of the Gaussian part of our multi-component fit to deduce the total spectral power of solar-type pulsation which is believed to scale with the luminosity-mass ratio. This, however, needs extensive calibration for solar-type pul-

Table 2. Our total sample of 31 analyzed pulsating red giants from the CoRoT LRc01 campaign. The frequency of maximum power, ν_{\max} , and the large frequency separation, $\Delta\nu$, are obtained from the power spectra of the photometric time series. Mass and radius are determined from Eqs. 4 and 5. The effective temperatures and luminosities are based on interpolation in a set of solar calibrated evolutionary tracks.

	CoRoT-ID	V [mag]	ν_{\max} [μ Hz]	$\Delta\nu$ [μ Hz]	R/R $_{\odot}$	M/M $_{\odot}$	T $_{\text{eff}}$	L/L $_{\odot}$
A	101113062	13.46	73.14	7.16	7.7 \pm 0.5	1.3 \pm 0.3	4662	24.8
B	101251252	13.72	65.30	6.58	8.2 \pm 0.5	1.3 \pm 0.3	4605	24.0
C	101362522	13.90	54.70	5.52	9.7 \pm 0.6	1.5 \pm 0.3	4641	38.6
D	101034881	13.50	46.50	4.78	11.0 \pm 0.7	1.7 \pm 0.3	4612	46.6
E	101197556	13.35	36.40	3.77	13.9 \pm 0.8	2.1 \pm 0.4	4591	68.9
F	100838545	12.76	30.70	3.78	11.6 \pm 0.7	1.2 \pm 0.2	4449	43.3
G	101649216	12.46	20.20	2.53	17.1 \pm 1.0	1.8 \pm 0.3	4469	109.0
H	101378942	12.76	14.60	1.98	20.2 \pm 1.2	1.8 \pm 0.3	4388	136.2
	101290847	13.20	59.55	6.20	8.4 \pm 0.5	1.3 \pm 0.2	4621	28.9
	101509360	13.06	54.25	5.76	8.8 \pm 0.5	1.3 \pm 0.2	4604	31.5
	101081290	12.73	51.55	5.42	9.5 \pm 0.6	1.4 \pm 0.3	4609	36.5
	101041814	13.51	43.14	4.96	9.5 \pm 0.6	1.2 \pm 0.2	4540	34.2
	100886873	13.57	41.34	4.73	10.0 \pm 0.6	1.2 \pm 0.2	4545	38.2
	100483847	12.70	40.41	4.45	11.1 \pm 0.7	1.5 \pm 0.3	4573	47.9
	101232297	12.48	39.95	4.85	9.2 \pm 0.6	1.0 \pm 0.2	4502	31.2
	100974118	13.74	39.52	3.87	14.3 \pm 0.9	2.4 \pm 0.5	4700	89.2
	100716817	13.86	36.60	4.14	11.6 \pm 0.7	1.5 \pm 0.3	4549	51.4
	101218811	13.46	36.03	3.99	12.3 \pm 0.7	1.6 \pm 0.3	4569	58.8
	101242228	13.10	33.16	3.97	11.4 \pm 0.7	1.3 \pm 0.2	4506	47.8
	101136306	12.61	33.07	3.98	11.3 \pm 0.7	1.3 \pm 0.2	4503	46.9
	101058180	12.61	32.85	4.09	10.6 \pm 0.6	1.1 \pm 0.2	4478	40.8
	100908597	13.95	32.48	3.86	11.8 \pm 0.7	1.4 \pm 0.3	4510	51.9
	101262795	14.16	30.16	3.88	10.8 \pm 0.7	1.1 \pm 0.2	4451	41.4
	101044584	13.00	28.68	3.19	15.2 \pm 0.9	2.0 \pm 0.4	4569	90.61
	101513442	14.32	27.42	3.73	10.6 \pm 0.6	0.9 \pm 0.2	4406	38.3
	100855073	14.13	26.78	3.30	13.3 \pm 0.8	1.4 \pm 0.3	4475	64.1
	101150795	14.11	25.98	3.15	14.1 \pm 0.9	1.5 \pm 0.3	4484	72.6
	101654204	13.59	25.78	3.33	12.6 \pm 0.8	1.2 \pm 0.2	4445	55.7
	100998571	13.70	25.59	2.99	15.5 \pm 0.9	1.8 \pm 0.4	4522	89.8
	101449976	12.38	23.03	2.83	15.5 \pm 0.9	1.7 \pm 0.3	4472	86.7
	101029979	14.64	21.85	2.60	17.5 \pm 1.1	2.0 \pm 0.4	4504	112.5

sators with independently determined fundamental parameters, which we currently carry out. If possible, and we have strong evidence for that, we can finally derive all basic fundamental parameters (mass, radius, luminosity, and consequently also the effective temperature) of a solar-type pulsator by simply measuring global properties of its pulsation power excess in the power density spectrum. This will have influence on various astrophysical applications. One can use it as a distance indicator, or one can study the behavior of convective time scales of stars as a function of their position in the HR-diagram. By comparing the individual pulsation frequencies with theoretical eigenfrequencies it should be possible to investigate the parameterization of convective models (e.g. the mixing length parameter in the mixing length theory) in a region of the HR-diagram where stars are very sensitive to these parameters.

Finally, we want to mention that we will apply our asteroseismic fundamental parameter determination to all pulsating red giants observed by CoRoT and we plan to arrange an online database for them.

Acknowledgements. T.K and W.W.W. are supported by the Austrian Research Promotion Agency (FFG), and the Austrian Science Fund (FWF P17580). JDR and FC are postdoctoral fellows of the Fund for Scientific Research, Flanders. APH acknowledges the support grant 500W0204 from the Deutsches Zentrum für Luft- und Raumfahrt e. V. (DLR). SH acknowledges financial support from the Belgian Federal Science Policy (ref: MO/33/018). Furthermore, it is a plea-

sure to thank D. Stello (University of Sydney) for providing us with the photometric data of M67.

References

- Aigrain, S., Favata, F., & Gilmore, G. 2004, *A&A*, 414, 1139
- Baglin, A. 2006, The CoRoT mission, pre-launch status, stellar seismology and planet nding (M.Fridlund, A.Baglin, J.Lochar and L.Conroy eds, ESA SP-1306, ESA Publication Division, Noordwijk, The Netherlands)
- Barban, C., Matthews, J. M., De Ridder, J., et al. 2007, *A&A*, 468, 1033
- Bedding, T. R., Butler, R. P., Kjeldsen, H., et al. 2001, *ApJ*, 549, L105
- Bouchy, F., Bazot, M., Santos, N. C., et al. 2005, *A&A*, 440, 609
- Carrier, F., Kjeldsen, H., Bedding, T. R., et al. 2007, *A&A*, 470, 1059
- Cox, J. P. 1980, *Theory of stellar pulsation* (Princeton University Press)
- Demarque, P., Guenther, D. B., Li, L. H., Mazumdar, A., & Straka, C. W. 2007, *Ap&SS* (arXiv:0710.4003), 447
- De Ridder, J., Barban, C., Baudin, F., et al. 2008, *Nature*, submitted
- Eggenberger, P., Charbonnel, C., Talon, S., et al. 2004, *A&A*, 417, 235
- Frandsen, S., Carrier, F., Aerts, C., et al. 2002, *A&A*, 394, L5
- Guenther, D. B., Demarque, P., Kim, Y.-C., & Pinsonneault, M. H. 1992, *ApJ*, 387, 372
- Harvey, J. 1985, in *ESASpecial Publication, Vol. 235, Future Missions in Solar, Heliospheric & Space Plasma Physics*, ed. E.Rolfé & B.Batrick, 199
- Hekker, S., Aerts, C., De Ridder, J., Carrier, F. 2006, *A&A*, 458, 931
- Kallinger, T., Guenther, D. B., Matthews, J. M., et al. 2008, *A&A*, 478, 497
- Kallinger, T., PhD thesis, 2008, University of Vienna, Austria
- Michel, E., Samadi, R., Baudin, F., et al. 2008, *A&A* (arXiv:0809.1078v1)
- Kjeldsen, H., Bedding, T. R., Viskum, M., Frandsen, S. 1995, *ApJ*, 109, 1313
- Kjeldsen, H., Bedding, T. R. 1995, *A&A*, 293, 87
- Kjeldsen, H., Bedding, T. R., Butler, R. P., et al. 2005, *ApJ*, 635, 1281

- Martic, M., Lebrun, J.C., Schmitt, J., et al. 2001, *ESASP*, 464, 431
Stello, D., Kjeldsen, H., Bedding, T. R., Buzasi, D. 2006, *A&A*, 448, 709
Stello, D., Bruntt, H., Kjeldsen, H., et al. 2007, *MNRAS*, 377, 584
Toutain, T., Fröhlich, C. 1992, *A&A*, 257, 287